A Review of Different Mascon Approaches for Regional Gravity Field Modelling since 1968

Markus Antoni

Institute of Geodesy, University of Stuttgart, Geschwister-Scholl-Str. 24D, D-70174 Stuttgart, Germany

Correspondence: M. Antoni (markus.antoni@gis.uni-stuttgart.de)

Abstract. The geodetic and geophysical literature shows an abundance of mascon approaches for modelling the gravity field of Moon or Earth on global or regional scale. This article illustrates the differences and similarities of the methods, which are labelled as mascon approaches by their authors.

Point mass mascons and planar disc mascons were developed for modelling the Lunar gravity field from Doppler tracking data. These early models had to consider restrictions in observation geometry, computational resources or geographical pre-knowledge, which influenced the implementation. Mascon approaches were later adapted and applied for the analysis of GRACE-observations of the Earth's gravity field with the most recent methods based on the simple layer potential.

Differences among the methods relate to the geometry of the mascon patches and in the implementation of the gradient and potential for the field analysis and synthesis. Most mascon approaches provide a direct link between observation and mascon parameter —usually the surface density or the mass of an element—, while some methods serve as a post processing tool of spherical harmonic solutions. This article provides an historical overview of the different mascon approaches and sketches their properties from theoretical perspective.

Keywords. regional gravity field analysis, mascon approach, point mass modelling, simple layer potential, post processing

1 Introduction

Studies of the early Lunar orbiters demonstrated significant orbit disturbances, which were traced back to an irregular Lunar gravity field. The term "*mascon*" was introduced by Muller & Sjogren (1968b) for describing these mass concentrations near the surface. In the same work, the name mascon was also introduced for the mathematical modelling of these mass concentrations. The concept was applied for several years to the gravity field of the Moon, as the method was capable of the nearside restriction of data in opposite to spherical harmonic solutions. The interest of regional modelling of the Earth's gravity field significantly increased since the gravity field mapping mission GRACE (2002–2017) and its successor mission GRACE-FO (2018 – present). The new observations enabled the analysis of temporal variations caused by water and ice masses redistribution, where regional gravity field modelling overcomes the spherical harmonic solutions. Hence, the mascon concept has been adapted and applied to Earth-related data by several research groups, either for regions of interest (Luthcke et al., 2008; Schrama et al., 2014; Ran et al., 2018) or on global scale (Koch & Witte, 1971; Andrews et al., 2015; Save et al., 2016).

A closer inspection of the publications, however, shows a variety of approaches under the label of mascons. This article shall give a historical overview of the most prominent representatives and an adequate definition of the mascon base functions. All different meanings of the investigated mascon approaches can be covered by the following definition: *The term mascon either refers to the fact of a significant gravitational anomaly within a celestial body, or to a modelling of these anomalies by localizing base functions. The localizing base functions which are labelled as mascons include point masses or discrete surface elements based on the simple layer potential. In case of surface elements, the surface density is constant per mascon and each localizing base function is —in a spectral representation at least in the limit of high degree expansion— a two-dimensional step function on the sphere. Methods of post processing are also labelled*

as mascon approach when their surface elements have a constant surface density. The shape of the mascon is not relevant for the definition and the surface of the celestial body is not necessarily covered.

This publication is focused on the mascons' definitions and will ignore other processing steps, like back-ground models, regional constraints or regularization techniques. Each mascon approach is presented by the associated gravitational potential of a single element and its gradient in the notation of representative literature. Properties of each approach are deduced from the theoretical perspective only, but without treating programming experiments or numerical aspects. Such a detailed and comprehensive review of the different mascon approaches can not be found in literature to our knowledge.

In several previous articles, the authors quote only the original publication (Muller & Sjogren, 1968b) for the term *mascon* and restrict themselves in the following texts to a specific mascon approach with its literature (e.g.: Luthcke et al. (2008); Lemoine et al. (2007); Krogh (2011); Andrews et al. (2015)).

A point mass model and planar discs are applied for modelling the Lunar gravity field in (Wong et al., 1971) and both methods are considered as mascon approaches. In (Watkins et al., 2015; Save et al., 2016) different mascon approaches are presented in the introductions, but without formulas or historical background. The authors of both articles classify three principle concepts:

A) Mascons which have an analytical expression for the gravitational potential and explicit partial derivatives for the gradient.

B) Mascons which are represented by a finite series of spherical harmonic functions and with partial derivatives derived via the chain rule.

C) Mascons which serve as a post-processing tool to obtain regional mass changes from monthly spherical harmonic solutions.

An analogous classification with additional literature is presented by (Abedini et al., 2021a), whose contribution is a numerical method for the gradient, which does not fit into the threefold scheme.

Many recent publications are related to mascon solutions either of the NASA Goddard Space Flight Center (GSFC) or of the Jet Propulsion Laboratory (JPL) or the Center for Space Research (CSR). The current JPL solutions are spherical cap mascons with analytical partial derivatives — i.e. category A in the classification— which are presented in Section 3.2. The mascon approaches of GSFC and CSR are based on spherical harmonic functions and they are a prominent example of type B (cf. Section 3.1). The mascon visualization tool at the University of Colorado Boulder (https://ccar.colorado.edu/grace/index.html) enables an analysis and comparison of the latest solutions at JPL and GSFC for regions and generates time series per location.

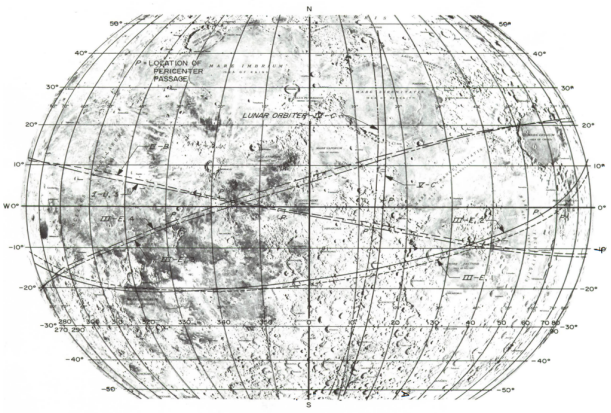

Figure 1. Lunar marias and selected tracks of Lunar Orbiter given in (Muller, 1972)

2 Mascons for modelling the Lunar gravity field

2.1 Mascons – mass anomalies close to the Moon's surface

The origin of the mascon concept is closely related to early models of the Lunar gravity field.

In the space race between the Soviet Union (USSR) and the United States of America (USA), both nations wanted to send their representatives to the Moon first. The possible landing sites were investigated by spacecrafts, starting with Luna 1 (USSR) in 1959, which missed the Moon due to navigation issues. The first man-made object on Moon was the space probe Luna 2 (USSR) in a design impact in 1959, followed by several missions of both nations. The spacecraft Luna 10 (USSR) and Lunar Orbiter 1 (USA) were the first artificial orbiters around the Moon in 1966 (Neal, 2008).

In both orbiter missions, the observed orbits differed after short time from the predicted ones, which indicated either an incorrect or an incomplete model. As other error sources could be excluded soon, the orbit disturbances were explained by significant mass anomalies below the Moon's surface. For these anomalies, the term "*mass concentration*" or "*mascon*" was introduced in (Muller & Sjogren, 1968b).

All identified mascons on the nearside of the Moon cause relatively large and positive effects up to $200\,\mathrm{mGal}$ and their locations are one-to-one correlated to the major Lunar maria including Imbrium, Serenitatis, Crisium, Humorum and Nectari, which are visualized in Fig. 1 (Muller, 1972).

In particular for the Moon it is still common to call a large area with a significant positive mass anomaly a mascon independent of its mathematical representation (Floberghagen, 2001, p.3). A similar behavior can be found for example in (Barthelmes, 1986, p. 35), where the mass anomalies of

the Earth gravity field are called mascons without using the phrase for the mathematical modelling as well. This thesis focuses on the point mass modelling, but it also sketches simple layer potential with discrete surface elements, and both aspects will be identified as mascon approaches in the current article.

Analyzing gravitational anomalies of a celestial body can provide information about its origin and physical processes, but the modelling is also helpful for the navigation of future space missions. An analysis by spherical harmonic functions is preferable for spherical bodies, as these base functions are the natural solution of the Laplace equation. However, a reasonable spherical harmonic analysis requires orbit observations with global and homogeneous data distribution. This requirement cannot be obtained by observations from terrestrial stations[1] towards Lunar orbiters due to the bounded rotation of the Moon and the observation geometry. Alternative localizing base functions like point masses are capable of irregular data distributions and they are applied for modelling the Lunar gravity field since 1968.

2.2 Point mass mascons

A quick modelling of the mass anomalies was important for the preparation of the latter space missions and the landing on the Moon. The chosen representation should

- consider the geographical pre-knowledge i.e. the Lunar maria as expected locations of the mass anomalies,
- consider the observation geometry, i.e. the fact that only the near side of the Moon allows observations from terrestrial ground stations,
- enable a direct relation between observables —Doppler tracking data in case of the early Lunar missions— and the estimated mascon parameters,
- remain simple due to limited computer resources.

The first three requirements are still important arguments for regional gravity field analysis — by mascons, wavelets, radial basis functions, Slepian functions etc.— , while the limited resources implied a simple modelling of the anomalies by point masses.

The original papers (Muller & Sjogren, 1968b, a; Muller, 1972) lack a formula representation of the potential, but it is re-constructed for example in (Floberghagen, 2001, p.19):

$$V(\mathbf{r}_P) = GM\left(\frac{1}{\|\mathbf{r}_P\|} - \sum_{q=1}^{Q}\frac{\delta m_q}{\|\mathbf{r}_P - \mathbf{r}_q\|}\right) \tag{1}$$

with

- $V(\mathbf{r}_P)$: gravitational potential at the calculation point $\mathbf{r}_P$,
- G: gravitational constant,
- M: mass of the celestial body,
- δm_q: mass ratio between point masses and total mass M,
- $\mathbf{r}_q$: centres of the point masses.

Please note, that for consistency all mascon quantities and their geometries are labelled in this article by an index (here: $q = 1, 2, ..., Q$), and the calculation point is labelled by the index P, both independent of the cited articles.

2.2.1 Relation to the observation and the estimation process

A standard observation technique for space probes is the Doppler tracking, i.e. the change in frequency of a (re)-transmitted signal due to relative motion of the satellite and the ground station. The American missions use a few globally distributed stations, which meanwhile form the Deep Space Network of the NASA and which are operated by JPL today[2]. The Doppler signal does not provide complete information on the position or velocity, but only a projection of the relative velocity between station and space probe onto the line-of-sight (Muller & Sjogren, 1968a; Weinwurm, 2004; Floberghagen, 2001).

The relationship between observation and mascon parameters requires a description of the change in velocity —i.e. the acceleration— of the spacecraft caused by the gravitational potential. Hence, it is sufficient to derive the gradient by $\ddot{\mathbf{r}}_P = \nabla V(\mathbf{r}_P)$ of the potential. For point mass model, the gradient is calculated via

$$\nabla V(\mathbf{r}_P) = GM\left(-\frac{1}{\|\mathbf{r}_P\|^3}\mathbf{r}_P + \sum_{q=1}^{Q}\frac{\delta m_q}{\|\mathbf{r}_P - \mathbf{r}_q\|^3}(\mathbf{r}_P - \mathbf{r}_q)\right). \tag{2}$$

To emphasize the special requirements and restrictions for the early Lunar modelling, some details shall be sketched here as well: According to (Muller & Sjogren, 1968a, b), residual observations are created by removing the gravitational effect of a tri-axial Moon model and the acceleration of Sun and other planets from the raw Doppler tracking data. Cubic polynomials are fitted to the residuals for smoothing and estimation of accelerations. The accelerations are mapped to a constant orbit height of 100 km altitude above the Moon's surface. The point masses are introduced directly below the trajectory with a depth of 50 km below the surface and their magnitudes are estimated. Additional information is given in (Wong et al., 1971), like the restriction

[1] A spherical harmonic analysis of the Earth's gravity field is possible even for ground-based observation, if the terrestrial station are well distributed.

[2] The equivalent system of the USSR is not discussed in the investigated material.

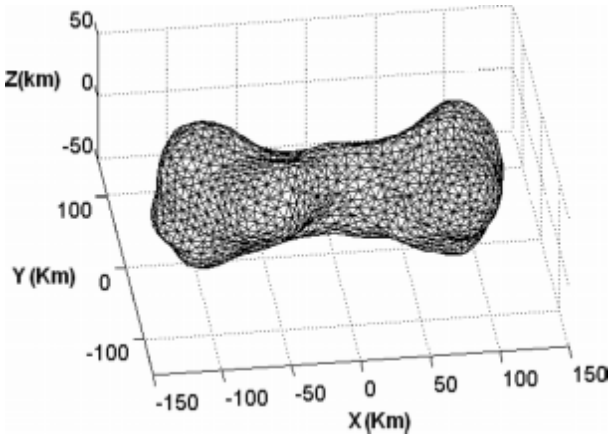

(a) Polyhedron model of the asteroid 216 aka Kleopatra

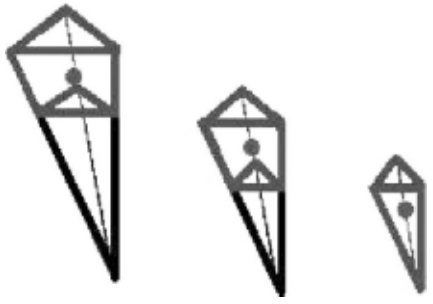

(b) Geometrically sub-division of one tetrahedron by parallel planes with the mascon locations as large dots

Figure 2. Modelling the gravity field of the asteroid Kleopatra by point mass mascons according to (Chanut et al., 2015), where the second image is converted to gray-scale for this article.

to 100 parameters in the estimation process due to implementation, and the step-wise solutions in North-South bands, which cover usually 8 trajectories —with 48 elements in the estimated state vectors— and around 50 point masses below the tracks.

2.3 Point mass mascons for irregular celestial bodies

Point mass mascons are also used in a different way to determine the gravity field of irregular celestial bodies. An example can be found in (Chanut et al., 2015), where the gravity field of the asteroid 216 – also known as Kleopatra – is predicted by polyhedron models and point mass mascons. In case of asteroids, the irregular shape is observed by optical instruments first, while orbiters investigate only in rare cases the gravity field directly. The observed shape is approximated by tetrahedrons with three corners on the surface and one in the geometrical centre of the asteroid (cf. Fig. 2a). Point masses are located then, either one per tetrahedron in its geometrical centre or three in the centres of a geometrically sub-divided tetrahedron (cf. Fig. 2b). Assuming a constant density of the asteroid and a known total mass, the mass per mascon is assigned to a value proportional to the surrounding volume and the gravity field around the object can be predicted.

Properties

The point mass mascons have closed formulas for potential and explicit partial derivatives, which identifies them as type A mascons in the threefold scheme:

+ The method is very easy to implement and requires only few computational resources.
+ The gradient and all other field quantities are found without quadrature.
– The model is singular for the potential and the gradient at the location of the point masses.
– In case of the Lunar gravity field, assumptions are required for location and depth below ground, as the Doppler tracking data and the observation geometry do not allow a detection of this information from the measurement.

It should be pointed out that the modelling by point masses is applied for example in (Baur & Sneeuw, 2011) or (Barthelmes, 1986; Claessens et al., 2001; Lin et al., 2014) without being labelled as mascon approach by the authors, and that in the latter examples also the positions of the masses are estimated for regional studies of the Earth's gravity field. An iterative algorithm is developed and justified via quasi-orthogonality in the sense of an inner product in (Barthelmes, 1986). To stabilize the optimization process, the possible movement per point mass shall be restricted in depth but also in radial or tangential direction w.r.t. to an initial position.

2.4 Planar disc mascons

As a response to (Muller & Sjogren, 1968b), an article of Conel & Holstrom (1968) presents a physical interpretation of the ringed Lunar maria, according to which former impact craters are filled afterwards by denser material. The authors experiment in the modelling of the mass anomalies with an arrangement of planar discs of finite thickness inside the impact craters and demonstrate a better post-fit to the residual Doppler tracking data for mare Serenitatis.

Obvious issues of point masses are discussed in (Wong et al., 1971), i.e

– the singularities of the model at the centres,
– bad fitting of the residual tracking data in the equatorial zone of the Moon due to the observation geometry,
– and combination issues with the spherical harmonic models (of very low degree and order at the time).

To overcome these problems, finite mass elements are suggested for modelling the gravitational anomalies, which also agrees with the physical ideas in (Conel & Holstrom, 1968).

The finite mass elements are chosen for a simple and efficient solution to be oblique rotational ellipsoids, also known as spheroids (Wong et al., 1971). The gravitational potential of a spheroid and its gradient are derived in (Moulton, 1960, p. 119–132). On the one hand, the gravitational potential requires a series expression

$$V = \frac{M}{R}\left[1 + \frac{b^2}{10}\frac{x_P^2 + y_P^2 - 2z_P^2}{R^4}e^2 + \mathcal{O}(e^3)\right] \tag{3}$$

with

- M: total mass of the spheroid (the gravitational constant is neglected in this exercise of the book),
- $R = \|\mathbf{r}_P\|$: Euclidean distance between spheroid's centre and calculation point $\mathbf{r}_P = (x_P, y_P, z_P)$ outside the body,
- b: semi-minor axis of the spheroid (and semi-major axis a),
- $e = \sqrt{\frac{a^2-b^2}{a^2}}$ numerical eccentricity.

On the other hand, the gradient of the potential can be derived in a closed formula. In (Wong et al., 1971), the semi-minor axis b is then squeezed to zero, which leads to the attraction of a circular and planar disc. The article provides the gradient of a single disc in the form

$$\begin{aligned}
\ddot{x} &= -\frac{3Gm}{2a^3}\left(\frac{-\sqrt{k}}{(1+k)} + \arcsin\left(\frac{1}{\sqrt{1+k}}\right)\right)x \\
\ddot{y} &= -\frac{3Gm}{2a^3}\left(\frac{-\sqrt{k}}{(1+k)} + \arcsin\left(\frac{1}{\sqrt{1+k}}\right)\right)y \\
\ddot{z} &= \frac{3Gm}{a^3}\left(\frac{1}{\sqrt{k}} - \arcsin\left(\frac{1}{\sqrt{1+k}}\right)\right)z,
\end{aligned} \tag{4}$$

where k fulfils the quadratic equation

$$k^2a^2 + \Big(a^2 - (x^2 + y^2 + z^2)\Big)k - z^2 = 0. \tag{5}$$

To bring the expressions of the gradient in (Moulton, 1960) and (Wong et al., 1971) into an analogous form, the identity $\arcsin\zeta = \arctan(\zeta/\sqrt{1+\zeta^2})$ must be kept in mind. It also turns out that the value k is linked to the numerical eccentricity of the spheroid by the relation $e = (1/\sqrt{1+k})$.

These planar disc mascons must be rotated and translated on the surface or close to it onto different locations, which is only implicitly indicated due to the definition of the coordinates (x, y, z) w.r.t. the centre of each disc (Wong et al., 1971).

Properties

The planar disc mascons have closed formulas for explicit partial derivatives of the potential, which identifies them as type A mascons:

+ The closed formulas don't require any integration for the gradient.
+ The surface elements have all the same shape, size and area for each mascon.
– The potential of a mascon requires a series expansion.
– The model is singular for the potential at the centre of the disc.
– The surface elements don't cover the complete surface even in a global analysis.
– Most points within a disc are either above or below the spherical surface.

In fact, the planar disc mascons are a kind of a simple layer potential, but without implicit or explicit integration for the gradient.

3 Simple layer potential and its regional subdivision

Modelling the gravitational potential by a simple layer was well known in geodesy and became popular around 1970.

The method can be applied to the complete potential or to a residual field after subtracting a reference field. The basic idea is to condensate the (remaining) in-homogeneous mass distribution onto the surface $\mathcal{S}$, either the topography itself or a simpler reference like a sphere or spheroid (Koch & Witte, 1971; Morrison, 1971).

The gravitational potential of the layer is given by

$$V(\mathbf{r}_P) = G\iint_{\mathcal{S}} \frac{\sigma(\Omega)}{\ell(\Omega, \mathbf{r}_P)}\mathrm{d}\Omega \tag{6}$$

with

- $V(\mathbf{r}_P)$: gravitational potential at the calculation point $\mathbf{r}_P$,
- $\sigma(\Omega)$: location dependent surface density,
- G: gravitational constant,
- $\ell(\Omega, \mathbf{r}_P) = \sqrt{(x_P - x)^2 + (y_P - y)^2 + (z_P - z)^2}$: Euclidean distance[3] between calculation point $\mathbf{r}_P = (x_P, y_P, z_P)$ and all surface points $\mathbf{P} = (x, y, z)$ with $\mathbf{P} \in \mathcal{S}$,

[3]The unusual arguments of the distance expressions are introduced here for highlighting the dependency on two distinct point sets.

– $\mathrm{d}\Omega$: the differential surface element.

In the mascon version of the simple layer potential, the surface $\mathcal{S}$ is sub-divided into smaller regions $\mathcal{S}_q$ —which are called surface elements or patches in this article—, where the density is assumed to be constant. This leads to the mascon representation of the (residual) potential

$$V_q(\mathbf{r}_P) = G\sigma_q \iint_{\mathcal{S}_q} \frac{1}{\ell(\Omega,\mathbf{r}_P)}\mathrm{d}\Omega \tag{7}$$

$$V(\mathbf{r}_P) = \sum_{q=1}^{Q} V_q(\mathbf{r}_P). \tag{8}$$

A linear combination (8) of all mascons —where the summation weights σ_q are included in the potential $V_q(\mathbf{r}_P)$ per mascon here— generates the potential of the simple layer again. On the one hand it should be pointed out, that the method is applied for example in (Koch & Witte, 1971) without being labelled as mascon approach. On the other hand, all following mascon approaches are based on the simple layer potential with discrete surface elements and constant surface densities which justifies the mascon label here as well.

3.1 Lumped spherical harmonics as mascons

Solving the Laplace equation in spherical coordinates leads to the spherical harmonic functions as a natural basis for gravity field modelling. An adequate linear combination of spherical harmonic functions can also be used to define localizing base functions like the mascons in the spectral domain. Due to this combination over all degrees and orders, the result is sometimes labelled as "*lumped spherical harmonic approach*" (Klosko et al., 2009).

Firstly, the gravity field is decomposed into a static field and its temporal variations:

$$V = V_0 + V_t \tag{9}$$

The static field and the mascons are represented by spherical harmonic synthesis. According to (Heiskanen & Moritz, 1967; Koch & Witte, 1971; Seeber, 2003), the potential is given by

$$V_0(\lambda_P,\theta_P,r_P) = \frac{GM}{r}\sum_{l=0}^{L}\left(\frac{R}{r}\right)^l \sum_{m=0}^{l}\overline{P}_{l,m}(\cos\theta_P) \times \left(\overline{C}_{l,m}\cos m\lambda_P + \overline{S}_{l,m}\sin m\lambda_P\right) \tag{10}$$

with

– $V_0(\lambda_P,\theta_P,r_P)$: potential of the static field,

– (λ_P,θ_P,r_P): spherical coordinates of the evaluation point $\mathbf{r}_P$, i.e. longitude λ_P, co-latitude θ_P and radius r_P,

– GM: product of gravitational constant G and the mass of the celestial body M,

– R: radius or semi-major axes of the spherical or ellipsoidal reference body,

– $\overline{P}_{l,m}(\cos\theta)$: fully-normalized Legendre functions,

– $\{\overline{C}_{l,m},\overline{S}_{l,m}\}$: fully-normalized spherical harmonic coefficients also known as Stokes coefficients.

The approach arised at GSFC when analysing the data of the GRACE-mission and it is presented in a sequence of articles (Rowlands et al., 2005; Lemoine et al., 2007; Klosko et al., 2009; Rowlands et al., 2010; Luthcke et al., 2013).

The mascons are generated in the spectral domain by (time-dependent) *delta Stokes coefficients* or *differential Stokes coefficients* of a simple layer

$$\Delta\overline{C}^q_{l,m}(t) = \frac{(1+k'_l)R^2}{(2l+1)M}\sigma_q(t)\iint_{\mathcal{S}_q}\overline{P}_{l,m}(\cos\theta)\cos m\lambda\mathrm{d}\Omega$$
$$\Delta\overline{S}^q_{l,m}(t) = \frac{(1+k'_l)R^2}{(2l+1)M}\sigma_q(t)\iint_{\mathcal{S}_q}\overline{P}_{l,m}(\cos\theta)\sin m\lambda\mathrm{d}\Omega \tag{11}$$

with the Love numbers k'_l for considering the loading effects of the extra masses on the surface.

The mascon solutions of the JPL are published online (https://earth.gsfc.nasa.gov/geo/data/grace-mascons), and also the mascon solution of the CSR can be found online (http://www.csr.utexas.edu/grace/). As the formulas require standard techniques of geoscience, also other groups are working with these kind of mascons (e.g. Andrews et al. (2015); Krogh (2011)).

The lumped spherical harmonic approach can be used for any (almost spherical) body, but the approach is in particular introduced for analysing the temporal variations of Earth's gravity field due to the variable water storage. Taking into account that a uniform layer of $1\,\mathrm{cm}$ fresh water within an area of $1\,\mathrm{m}^2$ has a mass of around $10\,\mathrm{kg}$, the density is rewritten in (Rowlands et al., 2010; Luthcke et al., 2013) as $\sigma_q = 10H_q$ —in (Save et al., 2016) the factor $\sigma_q = 10.25H_q$ is used instead— to express the results in centimetre of water height. Each mascon is determined by a spherical harmonic synthesis

$$H_q(\mathbf{r}_P,t) = \frac{M}{40\pi R^2}\sum_{l=0}^{L}\left(\frac{2l+1}{1+k'_l}\right)\sum_{m=0}^{l}\overline{P}_{l,m}(\cos\theta_P) \times \left(\Delta\overline{C}^q_{l,m}(t)\cos m\lambda_P + \Delta\overline{S}^q_{l,m}(t)\sin m\lambda_P\right) \tag{12}$$

on the spherical surface $r = R$ and with the upward continuation term $(R/r)^l$ in the synthesis formula if necessary.

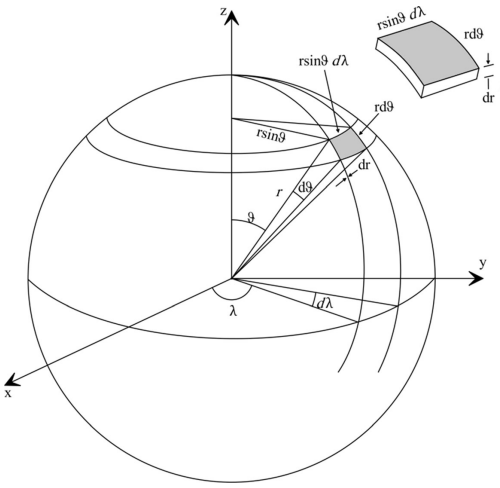

Figure 3. Sub-division in a longitude-latitude grid and a differential volume element of the sphere (Abedini et al., 2021a). In an alternative interpretation, the figure illustrates a two-dimensional step function on the sphere, which is either zero (=*white*) outside and constant but non-zero (=*gray*) inside a mascon element.

If the maximum degree L of the expansion is large enough, expression (12) forms a "two-dimensional step function" on the sphere $\mathcal{S}$ (cf. Figure 3) with

$$H_q(\mathbf{r}_P, t) = \begin{cases} H_q & \text{in the region of interest, i. e. } \mathcal{S}_q \\ 0 & \text{outside.} \end{cases} \qquad (13)$$

A straight-forward sub-division of a sphere is given by a longitude-latitude grid, i.e. all boundaries are either part of parallel circles or of meridians. In this case, the integrals (11) have the differential surface element $\mathrm{d}\Omega = \cos\theta \mathrm{d}\theta \mathrm{d}\lambda$ of the unit sphere and the integration can be obtained by recursion formulas of integrated Legendre functions.

The size and shape of the surface elements varies within the publications:

- (Lemoine et al., 2007; Rowlands et al., 2005) present a separation of the region of interest into surface elements of equal angles with the dimension $4° \times 4°$, while (Krogh, 2011) defines patches of the dimension $1.25° \times 1.5°$ and $1.5° \times 1.5°$.

- Equal areas within a longitude-latitude grid can be obtained by stretching or shrinking one of the angles dependent on latitude, which is discussed already in (Morrison, 1971), and applied in experiments of (Rowlands et al., 2010) and (Andrews et al., 2015).

- In (Klosko et al., 2009) the surface elements have — at least in the corresponding Figure 4— more complex boundaries. The lines are still along parallel circles and meridians, but combined in such a way, that the mascon patches fill irregular shapes of sub-basins within the Mississippi basin.

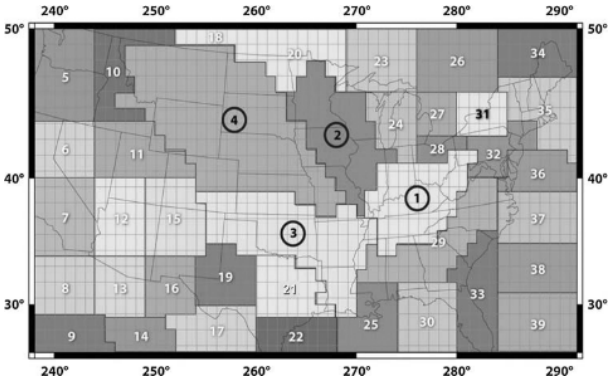

Figure 4. Definition of mascon surface elements in the Mississippi basin. The figure originates from (Klosko et al., 2009), but it is converted to gray-scale for this article.

- In the CSR solution, the equal area per mascon is considered to be more relevant than a simple sub-division or a complete coverage of the sphere (Save et al., 2016). A geodesic grid with 40962 vertices is generated by iteration, and the mascon patches are located in the centres. The shapes of the patches are either hexagonal or pentagonal, and the elements cover approximately equal areas of around $1°$ diameter.

The regularization techniques for equiangular patches are discussed (Abedini et al., 2021b) for another type of mascons, but the final recommendation to consider herein the area size should be transferable to the lumped spherical harmonic approach as well.

Observation of GRACE

The mascons were introduced for analysing the Earth's gravity field in the mission GRACE (Gravity Recovery And Climate Experiment). The mission consisted in two identical satellites, which were launched in 2002 in a cooperation of NASA/JPL and the German DLR. The satellites fell around the Earth in one common and almost circular orbit with a low altitude of originally $500\,\mathrm{km}$ height. The positions were quasi-permanently observed by GPS receivers with 3 antennas, and on-board accelerometers with three axis measured the combined influence of all non-gravitational effects. The main observable was the variation of the distance between the two GRACE satellites measured by microwaves in the K-band and Ka-band via a range-rate measurement system. The distance of $\rho \approx 250\,\mathrm{km}$ between the satellite centres varied due to mass variations below, and the K-Band provided a nominal accuracy of $10\,\mu\mathrm{m}$ for the range ρ, and $0.5\,\mu\mathrm{m/s}$ for the range-rate $\dot{\rho}$ (Seeber, 2003; Tapley et al., 2004).

The orbit observations and the gravity field parameters can be linked in different ways —e.g. the variational equation, the energy balance approach, the short arc approach or the acceleration approach— which are sketched for example in (Liu, 2008). The details are not in the focus of this work, but most methods require the gradient of the gravitational potential again.

Gradient of the lumped spherical harmonic mascons

For the range-rate $\dot{\rho}$ in the lumped harmonic approach, the relationship is found in (Luthcke et al., 2013) by chain rule

$$\frac{\partial \dot{\rho}}{\partial H_q} = \sum_{l=0}^{L} \sum_{m=0}^{l} \frac{\partial \dot{\rho}}{\partial \overline{C}_{l,m}} \frac{\partial \Delta \overline{C}^q_{l,m}}{\partial H_q} + \frac{\partial \dot{\rho}}{\partial \overline{S}_{l,m}} \frac{\partial \Delta \overline{S}^q_{l,m}}{\partial H_q} \tag{14}$$

and analogously for range-acceleration $\ddot{\rho}$. The derivatives $\left\{ \frac{\partial \Delta \overline{C}^q_{l,m}}{\partial H_q}, \frac{\partial \Delta \overline{S}^q_{l,m}}{\partial H_q} \right\}$ are straight-forward, as the formulas (11) are linear w.r.t. the surface density σ_q or the water height H_q.

Properties

The lumped spherical harmonic approach is a representative of the type B mascons.

+ The method is very easy to implement after a previous analysis of the GRACE-observations by spherical harmonic functions.
+ After the determination of all *delta Stokes coefficients*, all other field quantities can be calculated by standard methods of spherical harmonic synthesis.
+ The required integration (11) can be solved by well-known recursion formulas or by numerical quadrature.
– A high degree L of expansion might be required for straight boundaries and constant values within the two-dimensional step-functions.

3.2 Spherical cap mascons

The planar disc mascon approach (in Section 2.4) is not satisfying from a geometrical view point, as most points within the element are either above or below the spherical surface. This can be avoided by introducing spherical caps instead of planar discs. Monthly solutions in terms of spherical cap mascons are calculated at the JPL and the details can be found in (Watkins et al., 2015).

To reduce the effort of quadrature for the gradient expression, a *local mascon coordinate system* is introduced for each element by rotation where the centre of the mascon is equal to the new North pole of the system. The new coordinates are the spherical distance γ and the azimuth ξ in the calculation point. The potential is still based on the simple layer theory leading to the integral

$$\bar{V}_q(\mathbf{r}_P) = R^2 \sigma_q \int_0^{\alpha} \int_0^{2\pi} \frac{\mathrm{d}\xi \sin\gamma \mathrm{d}\gamma}{\ell(\Omega, \mathbf{r}_P)} \tag{15}$$

for the potential of a spherical cap with

– $\bar{V}_q(\mathbf{r}_P)$; gravitational potential per mascon in the local mascon coordinate system (the over-bar is introduced here to emphasize the rotated coordinate system),
– σ_q: product of the gravitational constant G and mass per mascon m_q divided by the area of the spherical cap, i.e. $\sigma_q = \frac{G m_q}{2\pi(1-\cos\alpha)R^2}$,
– R: radius of the spherical reference model,
– $\ell(\Omega, \mathbf{r}_P)$: distance between calculation point $\mathbf{r}_P = (x_P, y_P, z_P)$ and the points $\mathbf{P} = (x, y, z)$ in the spherical cap (in the original paper the Euclidean distance is unfortunately noted down by d),
– α: radius of the spherical cap in radians.

Gradient of the spherical cap mascons

The gradient of the potential $\bar{V}_q(\mathbf{r}_P)$ is calculated per mascon and rotated at the end to the original coordinate system. The iterated integration over the spherical distance and azimuth is reduced to a single integral by expressing the azimuthal component via elliptic integrals.

In the local mascon coordinate system, the gradient operator is of the form

$$\nabla \bar{V}_q = \left(\frac{\partial \bar{V}_q}{\partial r}, \quad 0, \quad \frac{1}{r} \frac{\partial \bar{V}_q}{\partial \theta} \right)^{\top} \tag{16}$$

where θ is the spherical distance between the calculation point and the mascon centre. The formulas of the gradient of a spherical cap are derived in an interoffice memorandum at the JPL (R. Sunseri (2010): *Mass concentration modelled as a spherical cap* 343R-11-00) —which is not available to us— and the results are quoted by (Watkins et al., 2015):

$$\begin{aligned} \frac{\partial V_q}{\partial r} &= -\sigma_q t^3 \left(\frac{I_2}{t} - \cos\theta \cdot I_1 - \sin\theta \cdot I_3 \right) \\ \frac{1}{r} \frac{\partial V_q}{\partial \theta} &= -\sigma_q t^3 \left(\sin\theta \cdot I_1 - \cos\theta \cdot I_3 \right) \end{aligned} \tag{17}$$

with the abbreviation $t = \frac{R}{r}$ and the three integrals $\{I_1, I_2, I_3\}$. The solution of the later ones requires complete elliptic integrals – first kind $\mathrm{E}(k)$ and second kind $\mathrm{K}(k)$ –

and numerical integration in the spherical distance direction

$$
\begin{aligned}
I_1 &= \int \sin\gamma\cos\gamma \left[\frac{m'}{\sqrt{l'+1}(l'+1)}\mathrm{E}(k)\right]\mathrm{d}\gamma \\
I_2 &= \int \sin\gamma \left[\frac{m'}{\sqrt{l'+1}(l'+1)}\mathrm{E}(k)\right]\mathrm{d}\gamma \\
I_3 &= \int \sin\gamma\cos\gamma \left[\frac{m'\Big(\mathrm{E}(k)-(1-l')\mathrm{K}(k)\Big)}{\sqrt{l'+1}(l'+1)l'}\right]\mathrm{d}\gamma
\end{aligned}
\tag{18}
$$

with the auxiliary expressions

$$
\begin{aligned}
n &= 1+t^2-2t\cos\theta\cos\gamma \\
m' &= 4/n^{3/2} \\
l' &= 2t\sin\theta\sin\gamma/n \\
k^2 &= 2l'/(l'+1).
\end{aligned}
\tag{19}
$$

Properties

The mascon potential is calculated by quadrature, and analytical derivatives have been derived, which leads to a class A mascon in the threefold scheme.

+ The two-dimensional quadrature for the gradients are reduced to a one-dimensional integration.
+ The calculation takes place only in the spatial domain and avoids the truncation error of spherical harmonic synthesis.
+ The surface elements have all the same shape, size and area for each mascon.
– The surface elements don't cover the complete surface even in a global analysis.
– The model is singular for the potential and the gradient at the location of the centre of the spherical cap.
– A straightforward implementation of the formulas (19) leads also to an undefined expression when the calculation point is identical to the centre of the spherical cap. One finds then $t=1$ and $\theta=0$ and in consequence $l'=0/0$. A solution might be given in the unavailable interoffice memorandum.

3.3 Mascons via quadrature of the simple layer potential

To avoid truncation errors and aliasing into coefficients of lower degree and order via the spherical harmonic expansion (14), a complete numerical integration is suggested in (Abedini et al., 2021a, b). The potential is represented —in our notation of Section 3— by the formula

$$
T(\mathbf{r}_P) = -G\iint_{\mathcal{S}} \frac{\sigma(\Omega)}{\ell(\Omega,\mathbf{r}_P)}\mathrm{d}\Omega \tag{20}
$$

and is evaluated by numerical quadrature when necessary. The extra minus-sign was likely introduced by the authors due to non-geodetic literature, as physical textbooks often use the definition $\ddot{\mathbf{r}} = -\nabla V$.

The derivatives of the range-rate $\dot\rho$ w.r.t. the surface density are quasi decomposed by the chain rule

$$
\frac{\partial\dot\rho}{\partial\sigma_q} = \frac{\partial\dot\rho}{\partial\mathbf{X}}\frac{\partial\mathbf{X}}{\partial\sigma_q} + \frac{\partial\dot\rho}{\partial\dot{\mathbf{X}}}\frac{\partial\dot{\mathbf{X}}}{\partial\sigma_q} \tag{21}
$$

into geometrical components $\left\{\frac{\partial\dot\rho}{\partial\mathbf{X}}, \frac{\partial\dot\rho}{\partial\dot{\mathbf{X}}}\right\}$ and dynamical components $\left\{\frac{\partial\mathbf{X}}{\partial\sigma_q}, \frac{\partial\dot{\mathbf{X}}}{\partial\sigma_q}\right\}$ with

– $\mathbf{X} = \mathbf{X}_2 - \mathbf{X}_1$: difference vector between the satellites' centre positions,
– $\dot{\mathbf{X}} = \dot{\mathbf{X}}_2 - \dot{\mathbf{X}}_1$: difference vector between the satellites' centre velocities.

As the range-rate $\dot\rho$ is calculated by $\dot\rho = \frac{\mathbf{X}^\top\dot{\mathbf{X}}}{\|\mathbf{X}\|}$, the geometrical components are known and can be differentiated w.r.t. positions and velocities.

The dynamical components are determined by the variational equation

$$
\ddot{\boldsymbol{\xi}} = \frac{\partial^2}{\partial t^2}\left\{\frac{\partial\mathbf{X}}{\partial\sigma_q}\right\} = \nabla^2 U(\mathbf{X})\frac{\partial\mathbf{X}}{\partial\sigma_q} + \frac{\partial\nabla T}{\partial\sigma_q} \tag{22}
$$

with $U = \frac{GM}{\|\mathbf{r}_P\|}$ being the potential of the Kepler problem. The equation is solved similarly to an orbit integration with the initial values $\boldsymbol{\xi} = \mathbf{0}$ and $\dot{\boldsymbol{\xi}} = \mathbf{0}$ for each arc, each satellite and each mascon. The integration error is limited by applying the method only to short arcs over the region of interest, e.g. Greenland in (Abedini et al., 2021a).

Properties

The approach is not fitting into the threefold scheme:

+ The method avoids truncation errors and aliasing by integration in the spatial domain.
+ The surface elements cover the complete surface in a global analysis.
– The potential and the gradient require numerical quadrature.
– The variational equations lead to a high computational burden, which is already admitted in (Abedini et al., 2021a).

4 Mascons as post processing tool

Since the successful GRACE-mission it is possible to observe also the temporal variations of the gravity field. The standard output of these investigations are monthly solutions of

spherical harmonic coefficients, which are meanwhile complemented by mascon solutions in the same time span by several research centres.

The question arises whether it is possible to estimate local variations from the spherical harmonic solutions by post processing. This is of particular interest for the ice masses and glaciers in Greenland, Antarctica, Alaska, and the highly variable water masses in the large water basins, which dominate the time-variable part of the gravity field.

The spherical harmonic functions have a global support, which contradicts a regional analysis. Another problem is the noise in the coefficients, which is overcome by filtering and de-striping techniques of the cost of the spatial resolution. To estimate regional mass changes, it can be helpful to determine an adequate field quantity by spherical harmonic synthesis and analyse this newly generated signal by another base function with local support (Ran et al., 2018).

4.1 Spherical cap mascon as a post processing tool

(Schrama et al., 2014) use the term mascon for post processing of a time series of Stokes coefficients $\{\bar{C}_{lm}(t), \bar{S}_{lm}(t)\}$. The goal is the determination of local mass variations in the ice shields and glaciers based on a time series of spherical harmonic coefficients.

A long-term mean value $\{\langle\bar{C}_{lm}\rangle, \langle\bar{S}_{lm}\rangle\}$ per coefficient is calculated and subtracted, and a Gauß-filter $W_l{}^{\mathrm{G}}$ in the spectral domain is applied by multiplication with the Stokes coefficients. To represent the equivalent water height instead of the potential, further standard factors are introduced:

$$\begin{Bmatrix} c^{\mathrm{w}}_{lm}(t) \\ s^{\mathrm{w}}_{lm}(t) \end{Bmatrix} = \frac{a_{\mathrm{e}}\rho_{\mathrm{e}}(2l+1)}{3\rho_{\mathrm{w}}(1+k'_l)} W_l{}^{\mathrm{G}} \begin{Bmatrix} \bar{C}_{lm}(t) - \langle\bar{C}_{lm}\rangle \\ \bar{S}_{lm}(t) - \langle\bar{S}_{lm}\rangle \end{Bmatrix} \tag{23}$$

with

- a_{e}: equatorial radius of the ellipsoidal Earth,
- ρ_{e}: mean density of the Earth,
- ρ_{w}: density of water,
- k'_l: Love numbers.

The spherical harmonic synthesis

$$h(\lambda_P,\theta_P,t) = \sum_{l=0}^{L}\sum_{m=0}^{l} \bar{P}_{lm}(\cos\theta_P) \times \left(c^{\mathrm{w}}_{lm}(t)\cos m\lambda_P + s^{\mathrm{w}}_{lm}(t)\sin m\lambda_P\right) \tag{24}$$

provides the mass variations w.r.t. a long term mean on a spherical surface. The equivalent water height $h(\lambda_P,\theta_P,t)$ is then analysed by a set of localizing base functions

$$h(\lambda_P,\theta_P,t) = \sum_{q=1}^{Q} \alpha_q(t)\beta_q(\psi_q,L,R) \tag{25}$$

via least squares estimation and the determination of the weights $\alpha_q(t)$. Each base function $\beta_q(\psi_k,L,R)$ has the form

$$\beta_q := \sum_{l=0}^{L} \gamma_l(R)\bar{P}_l(\cos\psi_q) \tag{26}$$

$$\gamma_l(R) = \frac{1}{2}\int_0^R \bar{P}_l(\cos\mu)\sin\mu\,\mathrm{d}\mu, \tag{27}$$

which is equivalent to a spherical cap with the radius R, the maximum expansion degree L in the spectral domain and the location (λ_q,θ_q) for its centre.

Properties

Original GRACE-data data are not required, as the method is applied on the previous solution by spherical harmonics, which leads to type C mascons:

+ The estimation of the weights is a straightforward process via least squares estimation.
+ The surface elements have all the same shape, size and area.
+ The required integration (27) can be solved by recursion formulas or numerical quadrature.
– The effect of Gauß-filtering and the temporal average on the solution's quality are difficult to predict, and also the chosen sampling in the spherical harmonic synthesis might have an effect on the estimated masses.
– The surface elements don't cover the complete surface even in a global analysis.

4.2 Point mass mascons as post processing tool

(Ran, 2017; Ran et al., 2018) extend an idea of (Baur & Sneeuw, 2011) by combining point masses and the simple layer potential. The goal of the work is the estimation of mass variations over Greenland based on spherical harmonic coefficients. The GRACE solutions are used to derive the radial component of the gradient but with loading compensation in orbit altitude:

$$\begin{aligned}\delta g(\mathbf{r}_P) &= -\frac{\partial V}{\partial r} \\ &= -\frac{GM}{r_P^2}\sum_{l=1}^{L}\frac{l+1}{1+k'_l}\left(\frac{a}{r_P}\right)^l \sum_{m=0}^{l}\overline{P}_{l,m}(\cos\theta) \\ &\quad\times\left(\Delta\overline{C}_{l,m}\cos m\lambda_P + \Delta\overline{S}_{l,m}\sin m\lambda_P\right).\end{aligned} \tag{28}$$

This signal is analysed —by least squares estimation of the surface densities ρ_q— by simple layer in the region of

interest:

$$\delta q_P = -\frac{\partial}{\partial r}\left\{ G\sum_{q=1}^{Q}\rho_q \iint \frac{\mathrm{d}s}{\ell(\Omega,\mathbf{r}_P)} \right\} = \\ = -\frac{\partial}{\partial r}\left\{ G\sum_{q=1}^{Q}\rho_q I_{q,p} \right\} \tag{29}$$

The integral $I_{q,p}$ is approximated by quadrature, which evaluates the distances only in the nodes of a grid

$$I_{q,p} = \iint \frac{\mathrm{d}s}{\ell(\Omega,\mathbf{r}_P)} \approx \sum_{j=1}^{K_q} w_{q,j}\frac{1}{l_{q,j,p}} \tag{30}$$

with

- $w_{q,j} = S_i/K_q$: weighting of the evaluated points,
- $l_{q,j,p}$: distance between the nodes and the evaluation point,
- S_q: the surface area of the mascon with the index q.

The Euclidean distance is expressed in spherical coordinates

$$l_{q,j,p} = \sqrt{r_{q,j}^2 + r_p^2 - 2r_{q,j}r_p\cos\Psi_{q,j,p}}$$

with

- $r_p = \|\mathbf{r}_P\|$: distance of calculation point to the origin,
- $r_{q,j} = \|\mathbf{r}_{q,j}\|$: distance of nodes within the patch to the origin,
- $\Psi_{q,j,p}$: angle between the vectors $\mathbf{r}_{q,j}$ and $\mathbf{r}_P$.

The observable of the study is then given by

$$\delta q_P \approx G\sum_{q=1}^{Q}\rho_q\sum_{j=1}^{K_q} w_{q,j}\frac{(r_{q,j} - r_p\cos\Psi_{q,j,p})}{{l_{q,j,p}}^3}. \tag{31}$$

Properties

The method is applied on the previous solution by spherical harmonics, which leads to type C mascons.

+ The method is very easy to implement.
+ Integration per mascon element is replaced by a weighted sum of point masses located on a grid.
- The model is singular for potential and radial derivative at the location of the nodes.
- Finding the weighting $w_{q,j} = S_i/K_q$ might be challenging for irregular shaped patches.

5 Summary – usage of mascons

Point mass models are an important tool for gravity field modelling due simplicity and efficiency. The representation is used for celestial bodies with irregular shapes, but also for Earth or Moon on regional and global scale. Point mass mascons are also a key aspect of converting spherical harmonic solutions into regional mass variations, which supports the interpretation of geophysical processes.

Mascons represented by finite surface elements are based on the simple layer potential. These models form a subset of localizing base functions for gravity field modelling. Without neighborhood conditions, a solution close to the ground generates a discontinuous field. The discontinuity problem is damped for higher evaluation altitude or small patches. The constant density per mascon simplifies the interpretation of mass variations in comparison to other localizing base functions (e.g. wavelets or Slepian functions), which vary within there region of interest. Planar disc and spherical cap mascons are radial symmetric base functions, while the other mascon concepts allow patches with arbitrary shapes. If the shapes consider the geometry of water basins, the leakage of signals can be reduced in hydro-geodesy.

Author contributions. M. Antoni: conceptualization, literature research, writing-original draft preparation, writing and editing.

Competing interests. The author declares that he has no known competing financial interests or personal relationship that could have appeared to influence the work reported in this paper.

Acknowledgements. The author is grateful to professor Nico Sneeuw at the Institute of Geodesy (University of Stuttgart) for encouraging and supporting the idea of an historical review.

References

Abedini, A., Keller, W. and Amiri-Simkooei, A.: Estimation of surface density changes using a mascon method in GRACE-like missions, Journal of Earth System Science **130**(1), https://doi.org/10.1007/s12040-020-01535-5, 2021a

Abedini, A., Keller, W. and Amiri-Simkooei, A. R.: On the performance of equiangular mascon solution in GRACE-like missions, Annals of Geophysics 64(2). https://doi.org/10.4401/ag-8621, 2021b

Andrews, S. B., Moore, P. and King, M. A.: Mass change from GRACE: a simulated comparison of Level-1B analysis techniques, Geophys J Int (200), pp. 503–518. https://doi.org/10.1093/gji/ggu402, 2015

Barthelmes, F.: Untersuchungen zur Approximation des äußeren Gravitationsfeldes der Erde durch Punktmassen mit optimierten Positionen, Ph.D thesis, Veröffentlichungen des Zentralinstituts für Physik der Erde 92, Potsdam,

https://gfzpublic.gfz-potsdam.de/pubman/item/item_236018_1/component/file_236017/barthelmes_diss1986.pdf, 122 pp., 1986

Baur, O. & Sneeuw, N.: Assessing Greenland ice mass loss by means of point-mass modelling: a viable methodology, J Geodesy 85, pp. 607–615. https://doi.org/10.1007/s00190-011-0463-1, 2011

Chanut, T. G. G., Aljbaae, S. and Carruba, V.: Mascon gravitation model using a shaped polyhedral source, MNRAS 450, pp. 3742–3749. https://doi.org/10.1093/mnras/stv845, 2015

Claessens, S., Featherstone, W., Barthelmes, F.: Experiences with Point-Mass Gravity Field Modelling in the Perth Region, Western Australia, Geomatics Research Australasia 75, pp. 53–86. http://hdl.handle.net/20.500.11937/317455, 2001

Conel, J. E. & Holstrom, G. B.: Lunar Mascons: A Near-Surface Interpretation, Science 162, pp. 1403–1405. https://doi.org/10.1126/science.162.3860.1403, 1968

Floberghagen, R.: The Far Side – Lunar Gravimetry Into the Third Millenium, Ph.D thesis, Technische Universiteit Delft, 283 pp., 2001

Heiskanen, W., & Moritz, H.: Physical Geodesy, W. H. Freeman, San Francisco, California, 1967

Klosko, S., Rowlands, D. D., Luthcke, S. B., Lemoine, F. G., Chinn, D. and Rodell, M.: Evaluation and validation of mascon recovery using GRACE KBRR data with independent mass flux estimates in the Mississippi Basin, J Geodesy 83, pp. 817–827. https://doi.org/10.1007/s00190-009-0301-x, 2009

Koch, K.-R. & Witte, B. U.: The Earth's Gravity Field Represented by a Simple Layer Potential from Doppler Tracking of Satellites, Technical report, U.S: Department of Comerce, 1971

Krogh, P. E.: High resolution time-lapse gravity field from GRACE for hydrological modelling, Ph.D thesis, Technical University of Denmark, 112 pp., 2011

Lemoine, F. G., Luthcke, S. B., Rowlands, D. D., Chinn, K. and Cox: The use of mascons to re-solve time-variable gravity from GRACE, in P. Tregoning and C. Rizos, eds, Dynamic Planet, Vol. 130 of International Association of Geodesy Symposia, Springer, Berlin Heidelberg, pp. 231–236, 2007

Lin, M., Denker, H. and Müller, J.: Regional gravity field modelling using free-positioned point masses, Stud Geophys Geod 58, pp. 207–226. https://doi.org/10.1007/s11200-013-1145-7, 2014

Liu, X.: Global gravity field recovery from satellite-to-satellite tracking data with the acceleration approach, Ph.D thesis, Delft, 226 pp., 2008

Luthcke, S. B., Arendt, A., Rowlands, D. D., McCarthy, J. J. and Larsen, C. F.: Recent glacier mass changes in the Gulf of Alaska region from GRACE mascon solutions, J Glaciol (188), pp. 767–777. https://doi.org/10.3189/002214308787779933, 2008

Luthcke, S. B., Sabaka, T., Loomis, B., Arendt, A., McCarthy, J. J. and Camp, J.: Antarctica, Greenland and Gulf of Alaska land-ice evolution from an iterated GRACE global mascon solution, J Glaciol (59)216, pp. 613–631. https://doi.org/10.3189/2013JoG12J147, 2013

Morrison, F.: Algorithms for Computing the Geopotential Using a Simple-Layer Density Model, Technical report, U.S: Department of Comerce, 1971

Moulton, F. R.: An Introduction to Celestial Mechanics, The Macmillian Company, New York. Second revised edition, fourteenth printing, 1960

Muller, P. M.: Implication of the lunar mascon discovery, in A. P. Society, ed., Proceedings of the American Philosophical Society, Vol. 116, pp. 362–364. https://www.jstor.org/stable/986067, 1972

Muller, P. M. & Sjogren, W. L.: Consistency of Lunar Orbiter Residuals With Trajectory and Local Gravity Effects, Technical Report Technical Report 32-1307, Jet Propulsion Laboratory, 1968a

Muller, P. M. & Sjogren, W. L.: Mascons: Lunar Mass Concentrations, Science 161, pp. 680–684. https://doi.org/10.1126/science.161.3842.680, 1968b

Neal, C. R.: The moon 35 years after Apollo: What's left to learn?, Chem Erde 69, pp. 3–43. https://doi.org/10.1016/j.chemer.2008.07.002, 2008

Ran, J.: Analysis of mass variations in Greenland by a novel variant of the mascon approach, Ph.D thesis, Delft University of Technology, 129 pp., 2017

Ran, J., Ditmar, P., Klees, R. and Farahani, H. H.: , Statistically optimal estimation of Greenland Ice Sheet mass variations from GRACE monthly solutions using an improved mascon approach, J Geodesy (92), pp. 299–319. https://doi.org/10.1007/s00190-017-1063-5, 2018

Rowlands, D. D., Luthcke, S. B., Klosko, S. M., Lemoine, F. G. R., Chinn, D. S., McCarthy, J. J., Cox, C. M. and Anderson, O. B.: Resolving mass flux at high spatial and temporal resolution using GRACE intersatellite measurements, Geophys Res Let 32(4). https://doi.org/10.1029/2004GL021908, 2005

Rowlands, D. D., Luthcke, S. B., McCarthy, J. J., Klosko, S. M., Chinn, D. S., Lemoine, F. G., Boy, J.-P. and Sabaka, T. J.: Global mass flux solutions from GRACE: A comparison of parameter estimation strategies – Mass concentrations versus Stokes coefficients, J Geophys Res-Sol 115(B1). https://doi.org/10.1029/2009JB006546, 2010

Save, H., Bettadpur, S. and Tapley, B. D.: High-resolution CSR GRACE RL05 mascons, J Geophys Res-Sol 121, pp. 7546–7569. https://doi.org/10.1002/2016JB013007, 2016

Schrama, E. J. O., Wouters, B. and Rietbroek, R.: A mascon approach to assess ice sheet and glacier mass balances and their uncertainties from GRACE data, J Geophys Res-Sol 119(7), pp. 6048–6066. https://doi.org/10.1002/2013JB010923, 2014

Seeber, G.: Satellite Geodesy (2. Edition), Walter de Gruyter, Berlin, New York, 2003

Tapley, B. D., Bettadpur, S., Watkins, M. and Reigber, C.: The Gravity Recovery and Climate Experiment: Mission Overview and Early Results, Geophys. Res. Lett. 31(9). https://doi.org/10.1029/2004GL019920, 2004

Watkins, M. M., Wiese, D. N., Yuan, D.-N., Boening, C. and Landerer, F. W.: Improved methods for observing Earth's time variable mass distribution with GRACE using spherical cap mascons, J Geophys Res-Sol 120(4), pp. 2648–2671. https://doi.org/10.1002/2014JB011547, 2015

Weinwurm, G.: Amalthea's Gravity Field and its Impact on a Spacecraft Trajectory, PhD thesis, Technische Universität Wien, 2004

Wong, L., Buechler, G., Downs, W., Sjogren, W., Muller, P. and Gottlieb, P.: A Surface-Layer Representation of the Lunar Gravitational Field', J Geophys Res, 76(26), pp. 6220–6236. https://doi.org/10.1029/JB076i026p06220, 1971